Separation Science and Technology
Publication details, including instructions for authors and subscription information:
http://www.informaworld.com/smpp/title~content=t713708471

The Effect of Particle Sedimentation on Gravity Filtration

Wei-Ming Lu; Kuo-Lun Tung; Chun-Hsi Pan; Kuo-Jen Hwang

To cite this Article Lu, Wei-Ming , Tung, Kuo-Lun , Pan, Chun-Hsi and Hwang, Kuo-Jen(1998) 'The Effect of Particle Sedimentation on Gravity Filtration', Separation Science and Technology, 33: 12, 1723 — 1746
To link to this Article: DOI: 10.1080/01496399808545902
URL: http://dx.doi.org/10.1080/01496399808545902

SEPARATION SCIENCE AND TECHNOLOGY, 33(12), pp. 1723–1746, 1998

The Effect of Particle Sedimentation on Gravity Filtration

WEI-MING LU,* KUO-LUN TUNG, and CHUN-HSI PAN
DEPARTMENT OF CHEMICAL ENGINEERING
NATIONAL TAIWAN UNIVERSITY
TAIPEI, TAIWAN 10617, REPUBLIC OF CHINA

KUO-JEN HWANG
DEPARTMENT OF CHEMICAL ENGINEERING
TAMKANG UNIVERSITY
TAMSUI, TAIPEI HSIEN, TAIWAN 25137, REPUBLIC OF CHINA

ABSTRACT

Simulation of cake formation of mono-sized and dual-sized particles under gravitational sedimentation and filtration is presented. The dynamic analysis proposed by Lu and Hwang in 1993 is applied to examine the local cake properties formed under a falling head by considering the hindered settling effect of particles in the slurry and the variation of the pressure drop across the filter septum. Results of this study show that, at a given position in a cake, the solid compressive pressure reaches a maximum value and then decreases for a gravity filtration due to the decrease in the driving head. A cake constructed with dual-sized particles has a more compact structure than does one with mono-sized particles, and larger particles will form looser packing than will smaller ones for mono-sized particles. A dual-dispersed suspension with a lower fraction of large particles will result in the lowest cake porosity and the highest specific filtration resistance of cake. Comparison of the porosity distribution in filter cake formed by means of gravity filtration and constant head filtration shows that the porosity near the filter septum of gravity filtration has a convex behavior while that of constant head filtration has a tendency toward concavity. This discrepancy is mainly due to the change in the driving head during the filtration process. Both theoretical and experimental results show that the uniformity of particle

* To whom correspondence should be addressed. Telephone: +886-2-23622707. FAX: +886-2-23623040. E-mail: wmlu@ccms.ntu.edu.tw

size distributions in the filter cake will be much better when the relative settling velocity between large and fine particles is reduced.

Key Words. Filtration; Gravity filtration; Local cake properties; Hindered settling effect; Dynamic analysis

INTRODUCTION

Gravity filtration and gravitational sedimentation are employed extensively in chemical and wastewater treatment processes to separate coarse solid particles from liquids in order to lower operating and capital costs and reduce maintenance. It was pointed out (1) that gravity filtration can also be used to determine cake resistance rapidly at low pressure in the laboratory. However, the effect of sedimentation is more serious in gravity filtration than in pressure filtration owing to the nonuniform size distribution of the particles in most slurries. Numerous researchers (2–5) have demonstrated that neglect of the sedimentational effect in pressure filtration or gravitational filtration will lead to underestimation of the mass of solids deposited in the cake and result in overestimation of the specific filtration resistance.

Gravity filtration under a falling head involves theoretical complications due to variations of the driving force and solid compressive pressure within the cake. To simplify the analysis, Nguyen (6) derived a numerical procedure for the gravity filtration process for a neutrally buoyant material, which eliminated the sedimentation effect during filtration and showed that the solid compressive pressure in the filter cake reaches a maximum value and then decreases. Tiller et al. (1) extended Nguyen's (6) work to obtain permeability and solidosity at low solid compressive pressures to facilitate the design of thickeners with compressed sediments. They compared the cake structure formed under gravitational filtration with those formed under free-settling and pressure filtration with negligible gravitational effects based on the derived mathematical formulations without any detailed explanation. Recently, Tiller et al. (5) took the effect of sedimentation into consideration for gravitational filtration and developed an approximation method based on a combination of traditional sedimentation and filtration theory in accordance with the CAT-SCAN data, which were used to estimate the relative settling velocity of particles in a fluid. They pointed out that the material balances of a filtration process based on the filtrate volume alone without corrections for the sedimentation effect will lead to a potentially large overestimate of the average specific resistance.

In this article the local cake structure formed under gravity filtration is analyzed theoretically by considering the effect of hindered settling of parti-

cles in the slurry and the variation of the pressure drop across the filter septum. Both mono- and dual-sized dispersion slurries are considered in this study, and the results of gravitational filtration are compared with experimental results obtained under sedimentation and constant head filtration for the same slurries.

ANALYSIS

During a course of gravity filtration, the liquid head falls as the filtration process proceeds, and the settling velocity of a particle in the slurry is impeded by the presence of other particles, resulting in a nonhomogeneous distribution of the slurry concentration along the filter column. In order to reveal the mechanism of gravity filtration, the dynamic analysis proposed by Lu and Hwang (7) is applied to evaluate the local cake properties formed under gravity filtration and is based on the following assumptions:

1. Solid particles and filtration liquid are incompressible.
2. No clogging of the filter medium by fine particles occurs during the filtration process.
3. The settling velocity of particles in the slurry can be calculated using Scott's (8) hindered settling model.
4. There are points of contact between solid particles.
5. Equilibrium porosity is attained instantaneously with changing pressure.

The pre-required input data include a set of experimental v vs t data from the course of gravity filtration, the resistance of the filter medium, and hindered settling coefficients.

Slurry Concentration Profile and Cake Surface Structure

Settling Velocity of Particles in Slurry

In gravity filtration the net velocity of particles in the slurry is the sum of the hindered settling velocity and the liquid velocity, that is,

$$u = U + q \tag{1}$$

For a polydispersed suspension, the settling velocity of particles under gravity can be estimated using the hindered settling model and can be expressed as

$$U = U_0 f(\phi) \tag{2}$$

where U_0 is the Stokes' velocity of the settling particles while $f(\phi)$, the hindered settling factor, is a function of the volume fraction of particles, ϕ. The empirical correlation proposed by Scott (8),

$$f(\phi) = (1 - \beta\phi)^{(4.70 + 17.8d^*/D)} \quad (3)$$

is a reliable model for estimating the laminar settling velocity for both deal suspensions of well-dispersed spheres and industrial suspensions. In Eq. (3), D is the diameter of the filter column, d^* is the mean volume-surface-length diameter of the settling particles (8), and the value of the hindered settling coefficient, β, can be extracted from the experimental data of sedimentation by regression. Although the hindered settling coefficient is a constant under all the conditions employed in the experimental work, Eq. (3) can be applied to a binary mixture of sedimenting particles based on the assumption that the hindering effect on a particle can be quantified simply by the total solid concentration surrounding the particle regardless of other characteristics of the suspension.

Concentration Profile in a Gravity Filter

Based on the estimated velocity of particles from Eq. (1), the concentration profile of particles can be calculated in a batch gravity filtration system. The initial coordinates of particles are determined by a numerical generator with a random distribution function. The slurry in a filter column is divided into several layers; then, the volume fraction of particles, ϕ, for each layer can be evaluated. From the velocity of particles calculated using Eq. (1), the displacement of particles in a time increment Δt can be estimated by integrating Newton's second law of motion. After each increment the position of each particle is determined and recorded, and the ϕ value of each layer is calculated afresh. By repeating these steps, the variations of the concentration profile and size distribution of the particles in each layer during a course of gravity filtration can be obtained.

Packing Structure of Particles and Porosity on Cake Surface

The three-dimensional particle-packing simulation method proposed by the authors (9) can be employed to estimate the packing porosity of particles on the cake surface. Based on a force balance model, the deposited position of each particle as well as the packing structure can be determined. When the simulation is completed, the porosity of the cake can be estimated accordingly. If the shape of the particles is not spherical, the porosity should be corrected using the shape factor of particles (7).

Dynamic Analysis on Local Cake Properties

During the course of cake filtration, the cake is compressed continuously by the frictional drag of the fluid. In this study an iteration process is estab-

lished to estimate the variations of the local cake properties, such as the local solid compressive pressure, porosity, specific filtration resistance, and particle size distribution in the cake.

Governing Equations

The Kozeny Equation. The well-known Kozeny equation for fluid flow through a porous medium can be expressed as

$$q = \left(\frac{dP}{dx}\right) \frac{\epsilon^3}{\mu k S_0^2 (1 - \epsilon)^2} \tag{4}$$

in which ϵ is the cake porosity, μ is the viscosity of the fluid, S_0 is the specific surface area of the particles, and k is the Kozeny constant. Since the value of S_0 largely depends on the particle size, it can be estimated as

$$S_0 = \int_{d_{p,min}}^{d_{p,max}} (6/d_p)\varphi(d_p)d(d_p)$$

for a cake formed by particles with nonuniform size distribution. The quantity $\varphi(d_p)$ is the mass fraction of particles of size d_p in the filter cake.

Kozeny Constant. Happel and Brenner (10) derived an expression for the relationship between the Kozeny constant and porosity as

$$k = \frac{2\epsilon^3}{(1 - \epsilon)\{\ln[1/(1 - \epsilon)] - [1 - (1 - \epsilon)^2]/[1 + (1 - \epsilon)^2]\}} \tag{5}$$

Thus, prior to employing Eq. (4) to estimate the flow rate of the filtrate or the pressure drop across the filter cake, the value of k should be corrected using the local cake porosity.

The Filtration Pressure Drop. In a falling head filtration, the hydrostatic pressure at the surface of the filter septum is determined by the sum of the liquid present in the pores of the cake, the slurry in region $(H_S - L)$, and in the no-solids region $(H_L - H_S)$ as shown in Fig. 1:

$$P(t) = \rho_l g L(t) + \rho_m(t) g[H_S(t) - L(t)] + \rho_l g[H_L(t) - H_S(t)] \tag{6}$$

where ρ_l and ρ_m are the densities of the liquid and slurry, respectively. The density of the slurry at time t can be calculated from

$$\rho_m(t) = \frac{w_l(t) + w_s(t)}{H_S(t) - L(t)} \tag{7}$$

where w_l and w_s are the liquid weight and solid weight per unit area in the slurry region, respectively, and they can be given as follows:

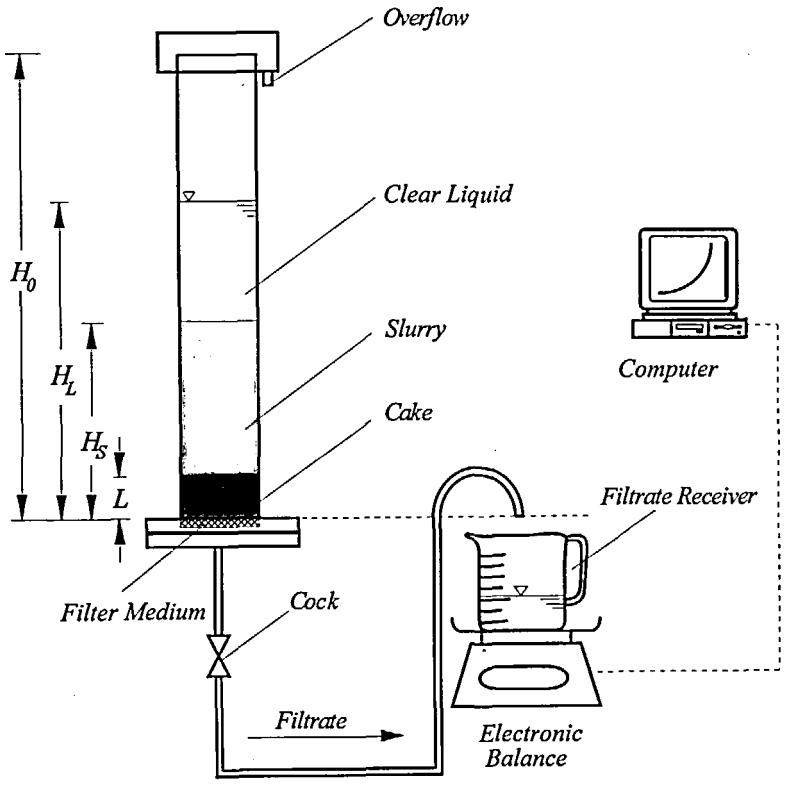

FIG. 1 A schematic diagram of batchwise gravity filtration.

$$w_l(t) = w_{l0} - \rho_l[H_0 - H_S(t)] - \rho L(t)\epsilon_{av}(t) \tag{8a}$$

and

$$w_s(t) = w_{s0} - \rho_s L(t)[1 - \epsilon_{av}(t)] \tag{8b}$$

in which w_{l0} and w_{s0} are the initial liquid weight and solid weight per unit area in the system, respectively, and ϵ_{av} is the averaged cake porosity.

Substituting Eqs. (7), (8a), and (8b) into Eq. (6), the hydrostatic pressure can be rearranged as

$$P(t) = \rho_l g\left\{H_L(t) + \frac{(\rho_{m0} - \rho_l)}{\rho_l} H_0 + L(t)[1 - \epsilon_{av}(t)]\left(1 - \frac{\rho_s}{\rho_l}\right)\right\} \tag{9}$$

where the initial density of slurry, ρ_{m0}, can be calculated by

$$\rho_{m0} = \frac{w_{l0} + w_{s0}}{H_0} \tag{10}$$

Then the pressure drop across the filter cake can be expressed as the difference of the applied hydrostatic pressure and the pressure required to overcome medium resistance, which is given by

$$\begin{aligned}\Delta P_c(t) &= P(t) - \Delta P_m(t) \\ &= \rho_l g\left\{H_L(t) + \frac{(\rho_{m0} - \rho_l)}{\rho_l} H_0 + L(t)[1 - \epsilon_{av}(t)]\left(1 - \frac{\rho_s}{\rho_l}\right)\right\} \\ &\quad - \mu q(t) R_m \end{aligned} \tag{11}$$

For constant head filtration, the liquid level remains constant during the filtration process; thus, the clear liquid level, $H_L(t)$, in Eq. (11) is replaced by the initial liquid height, H_0.

The Specific Filtration Resistance and Solid Compressive Pressure. Comparing Eq. (4) with the differential form of the cake filtration equation, the specific filtration resistance in the jth cake layer at $t = t_i$ as shown in Fig. 2 can be given as

$$\alpha_{i,j} = k_{i,j} S_{0_j}^2 \frac{(1 - \epsilon_{i,j})}{\rho_s \epsilon_{i,j}^3} \tag{12}$$

and the solid compressive pressure $P_{S_{i,j}}$ as

$$P_{S_{i,j}} = P(t) - \Delta P_m(t) - \sum_{n=1}^{j-1} \Delta P_{c_{i,n}} \tag{13}$$

Continuity Equation of Compression. Figure 2 illustrates the cake growth and compression in a gravity filtration system in which fluid flows from top to bottom, and where the distance is measured from the surface of the septum. For a given controlled mass (each layer of the cake), the continuity equation of compression is (11)

$$\left(\frac{\partial q}{\partial x}\right)_t = \left(\frac{\partial \epsilon}{\partial t}\right)_x \tag{14}$$

This equation can be employed to describe the relationship between the difference of the flow rate of the filtrate and the variation of cake porosity.

In this study it is assumed that no inter layer transport of particles occurs; i.e., a cake layer may be compressed but no transport of particles out of, or into, the layer is allowed. This assumption makes the value of $\Delta x_{i,j}(1 - \epsilon_{i,j})$ of cake layer j remain constant during filtration. Thus, the relationship be-

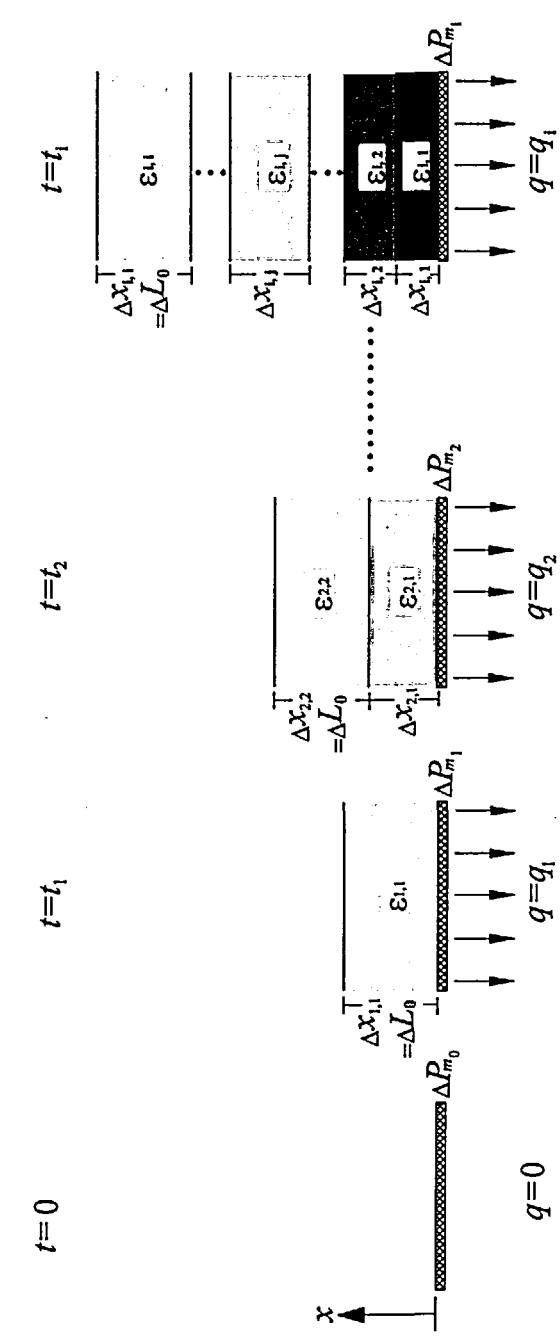

FIG. 2 A schematic representation of cake formation and compression in gravity filtration.

tween cake thickness and its porosity before and after compression can be represented as

$$\frac{\Delta x_{i+1,j}}{\Delta x_{i,j}} = \frac{1 - \epsilon_{i,j}}{1 - \epsilon_{i+1,j}} \tag{15}$$

By solving Eqs. (14) and (15), the variations of the cake porosity and the flow rate of the filtrate within the cake can be estimated.

The Known Conditions

The known conditions for the analysis and experimental measurements are summarized as follows.

Flow Rate of Filtrate, $q_{i,1}$. The instantaneous flow rate of filtrate can be obtained by differentiating the filtration data.

The Hindered Settling Coefficient, β. The value of the hindered settling coefficient, β, can be obtained by regression from the experimental data of sedimentation.

Porosity on Cake Surface, $\epsilon_{i,i}$. From the 3-D particle packing simulation, the variation of cake surface porosity can be obtained according to the slurry concentration and the fluid flow rate right upon the cake surface during a course of gravity filtration, and the ratio of wet to dry mass on the cake surface at time $t = t_i$, $m_{i,i}$ can be calculated accordingly. The cake surface porosity can also be obtained by means of a low head filtration system proposed by Haynes (12).

Filter Medium Resistance, R_m. In gravity filtration the pressure drop through the filter medium, ΔP_m, can not be neglected as it is in pressure filtration. If the resistance of the filter septum, R_m, can be assumed to remain constant during a course of filtration, then the value of R_m can be obtained by extrapolation of the filtration data $R_m = P|_{t=0}/(q|_{t=0} \cdot \mu)$, and the pressure drop of the flow of the fluid through the filter septum can be calculated accordingly.

Flow Rate of Fluid at Cake Surface, $q_{i,i}$. By taking a mass balance for the whole filter cake, the ratio of the fluid flow rate at the cake surface, $q_{i,i}$, to the fluid flow rate of the filtrate, $q_{i,1}$, for a course of variable pressure filtration can be expressed as (13):

$$\frac{q_{i,i}}{q_{i,1}} = \frac{\left[(1 - s)\left(1 - \epsilon_{av} - L\frac{d\epsilon_{av}}{dL}\right) - (m_{i,i} - 1)(1 - \epsilon_{i,i})s\right](1 - \epsilon_{av})}{(1 - m_{av}s)\left(1 - \epsilon_{av} - L\frac{d\epsilon_{av}}{dL}\right)(1 - \epsilon_{av}) - \left(\frac{\rho_l}{\rho_s}sL\frac{d\epsilon_{av}}{dL}\right)} \tag{16}$$

where s is the mass fraction of particles right at the cake surface, m_{av} is the average mass ratio of wet to dry cake, and $m_{i,i}$ is the mass ratio of wet to dry cake on the cake surface at time $t = t_i$.

Thickness of Instantaneously Formed Surface Cake Layer, ΔL_0. The instantaneous build up of the filter cake is caused by presetting a constant height of a newly formed cake layer. Then, as the porosity of the newly formed cake layers attain the value of the cake surface porosity, $\epsilon_{i,i}$, the instantaneous growth mass of the filter cake and its size distribution of particles can be obtained by calculating the particles which fall in the newly formed cake layer within the time interval.

Procedures to Analyze Local Cake Properties

Based on the pre-required input data and the governing equations mentioned above, the general sequence of an iteration process can be established to analyze the local cake properties and their variations in the course of gravity filtration. The procedure is described as follows.

(a) At the beginning of filtration, the initially formed cake layer has not been compressed yet; thus, the cake surface porosity, $\epsilon_{i,i}$, can be estimated by means of 3-D particle packing simulation. Then, one can calculate the total head, $P(t)$, using Eq. (9); the flow rate at the cake surface, $q_{1,i}$, using Eq. (4); the filtration pressure drop across the first cake layer, $\Delta P_c(t_1)$, using Eq. (11); and the specific filtration resistance of the first cake layer, $\alpha_{1,i}$, using Eq. (12).

(b) Before the second cake layer is formed, the concentration profile of particles in the slurry system is simulated based on Eq. (1), and the cake surface porosity, ϵ_i, can be estimated through 3-D particle packing simulation. When the porosity of the top layer equals the simulated value, the second cake layer can be regarded as having been formed, and the time t is denoted as t_2. From experimental data of the filtration rate, the value $q_{2,i}$ can then be calculated from Eq. (16). The total head at time $t = t_2$ is calculated using Eq. (9). The filtration pressure drop across the entire cake, $\Delta P_c(t_2)$, and the pressure drop of the fluid through the upper layer of the cake, $\Delta P_{c_{2,j}}$, are estimated using Eqs. (11) and (4), respectively. Ultimately, the pressure gradient through the bottom layer of the cake can be obtained from the difference of the total head and $\Delta P_{c_{2,j}}$. Substituting the pressure gradient into Eq. (4), the porosity of the bottom layer can be estimated. The profile of the hydraulic pressure and the average porosity of the cake can be calculated and used as the initially guessed values for the next iteration.

(c) The filter cake is divided into several layers of controlled mass. For each layer of cake, e.g., layer j, a smaller value of cake thickness is tried for

each iteration. Then its porosity is calculated by using Eq. (15), the flow rate of the filtrate using Eq. (16), and the pressure gradient using Eq. (4) until the calculated hydraulic pressure matches the assumed profile.

(d) For each time increment we repeat Step (c) until the total filtration pressure is equal to the pressure calculated using Eq. (11). If the calculated pressure does not match the applied pressure, the calculated profile of the hydraulic pressure is adopted for a new check condition to repeat Step (c).

(e) Substituting the local porosity of the cake into Eqs. (12) and (13), the values of the local specific filtration resistance and the solid compressive pressure for each layer of cake can be estimated.

(f) We repeat Steps (c) to (e) until filtration is accomplished. The variations of the local cake properties for the entire path of gravity filtration can be simulated.

EXPERIMENTAL

Gravity filtration, constant head filtration, and sedimentation were carried out using a filtration system as shown in Fig. 1. The filter column, with a height of 0.975 m and an inside diameter of 0.049 m, was made from transparent Plexiglas to facilitate observation of the slurry level and cake surface. In the course of constant head filtration, clear liquid was added to keep the driving head constant.

Two sizes of polystyrene beads with mean diameters of 365 μm (σ = 30 μm) and 225 μm (σ = 45 μm), respectively, were used in filtration experiments. The specific gravity of polystyrene is 1.07 and its shape is spherical.

In order to prevent aggregation of the particles during the process, the polystyrene beads were suspended in alcohol aqueous solution (67 vol% deionized water + 33 vol% ethanol) using a mixer to prepare the slurry before each experiment. The particles were sterically stabilized in the alcohol solution by solvated aliphatic chains grafted onto the particle surface. The adsorbed layer could be regarded as providing a barrier around each particle to prevent it from approaching other particles too closely.

As the slurry was poured into the filter column, filtration started immediately. The increase of the mass of the filtrate was detected by a load cell and recorded in a personal computer. The height of the slurry was observed through the transparent Plexiglas wall of the filter column. The thickness of the cake was recorded by a CCD camera which was installed parallel to the cake surface through the transparent Plexiglas wall of the filter column. Therefore, the average porosity of the filter cake could be calculated from the known volumes of the cake and filtrate.

After the filtration process was terminated, the wet filter cake was sliced into five equal layers parallel to the filter medium. They were analyzed to determine the particle size using a light-scattering particle size analyzer, Coulter LS-230.

RESULTS AND DISCUSSION

Simulated figures of three-dimensional gravity filtration and sedimentation processes with the same initial suspension composition are compared schematically in Fig. 3. These figures reveal that in the process of gravity filtration the interfaces of the suspension region fall and the cake builds up faster than in sedimentation.

These figures also show that the formation of cake by gravity filtration differs from that by sedimentation in both the thickness of filter cake formed and the nonuniformity of the particle size distribution in the filter cake. In sedimentation the effective drag acting on the particles is the result of the downward force of the buoyed weight of the particles minus the upward force of the friction due to the Darcian flow of liquid, while in gravity filtration the additional frictional drag due to liquid flow is added to the buoyed weight of the particles, which results in a cake more compact than sediment in the sedimentation process as shown in Fig. 3(c). Furthermore, it can be observed in these figures that the particle size distribution in a cake formed through gravity filtration is more uniform than that in the sediment formed in the sedimentation process due to fluid flow toward the septum, which reduces the relative settling velocity between large and fine particles.

Local Concentration Profile of Particles in Slurry Column

Figure 4 shows examples of the time course of the slurry concentration profiles during the gravity filtration and sedimentation processes of a dual-dispersed polystyrene suspension with $\omega = 75$ and $\phi_0 = 0.028$. The velocities of each particle were calculated using Eq. (2), and the coefficient β in Eq. (3) was obtained by means of a set of sedimentation experiments on a mono-dispersed suspension. For a mono-dispersed polystyrene suspension, the value of β obtained in this work by regression of the settling velocity of particles versus the volume fraction of particles was found to be 5.05. At the beginning of the processes the slurry concentration increased from the bottom of the column while the top was little affected. As an example of a time of $t = 20$ seconds in gravity filtration, since the large particles have higher settling velocities than do the fine particles, three zones form above the cake. From the top downward they are a clear liquid, a zone of variable composition, and a constant composition region (as the vertical line portion in Fig. 4 indicates). The rise of the end point

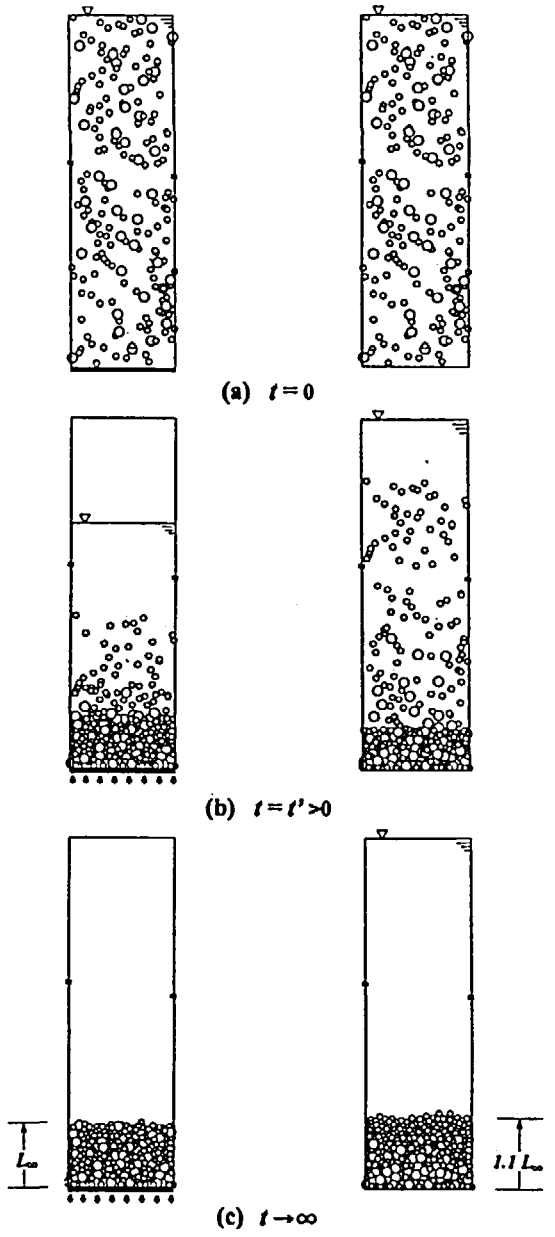

FIG. 3 A schematic diagram of a comparison of gravity filtration and sedimentation with sample slurry of $\omega = 50$ and $\phi_0 = 0.028$.

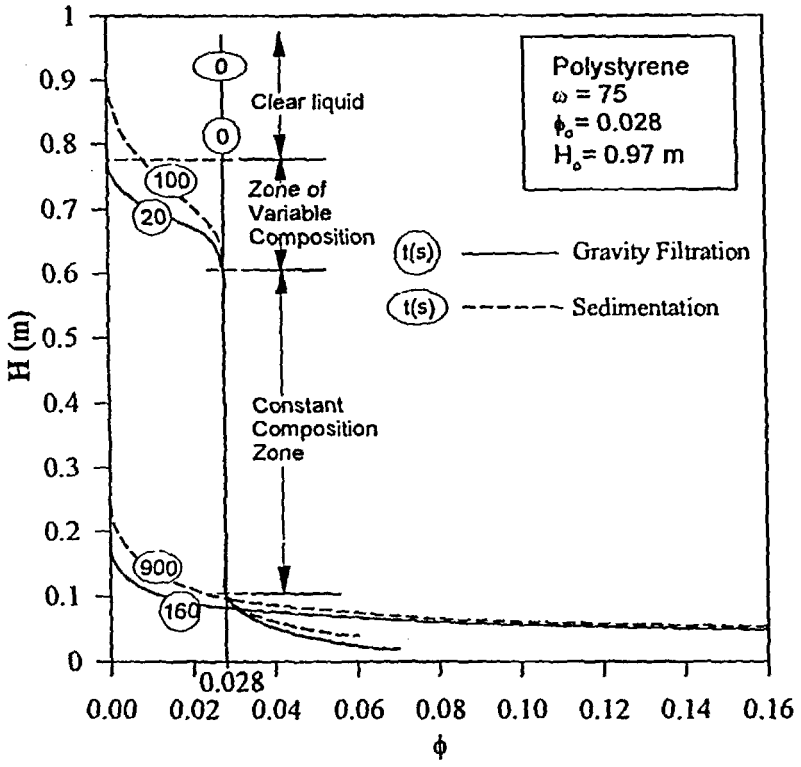

FIG. 4 Time course of the variation of the particle concentration profile in the slurry column.

of each curve for both gravity filtration and sedimentation denotes the increase of cake thickness with time. As shown in this figure, the nonuniformity of the particle concentration in the slurry column propagates downward along the cake surface as time increases. All the profiles have a concave shape near the cake surface. This indicates that there is a sharp increase of slurry concentration near the cake surface. On the other hand, comparison of the concentration curves of gravity and sedimentation reveals that the interface between the clear liquid and suspension region decreases faster in the course of gravity filtration compared with that in sedimentation.

Figure 5 shows an example of the concentration profiles of particles in the column with various weight percentages of large particles, ω, at $t = 75$ seconds in gravity filtrations. All of the suspensions have the same initial total volume fraction of particles, $\phi_0 = 0.028$. It is interesting to note that the interface between the clear zone and the slurry zone falls faster for a

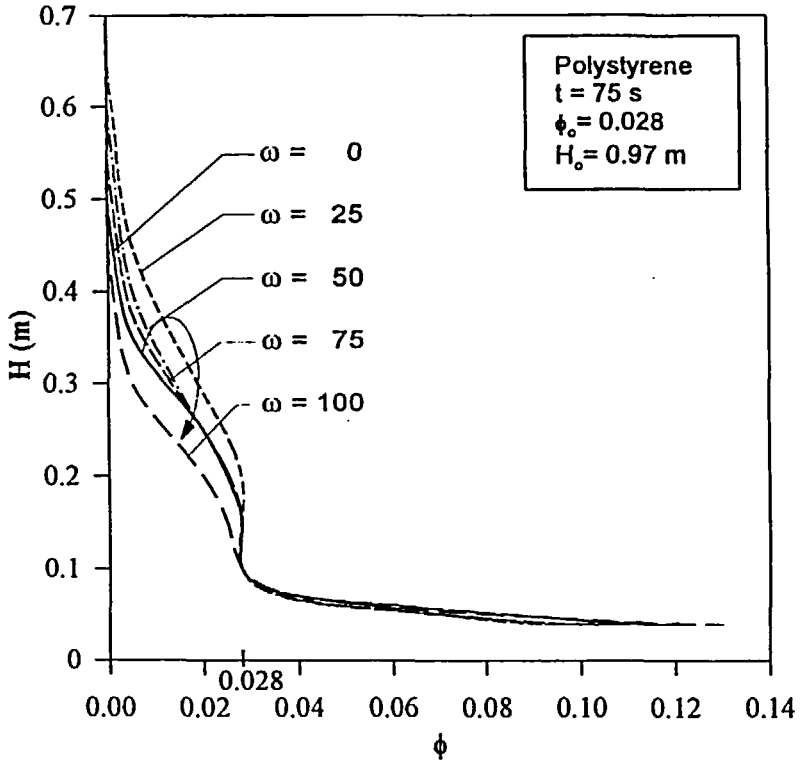

FIG. 5 Concentration profiles for different ω values at t = 75 seconds in gravity filtration.

larger value of ω. This occurs because the large particles fall faster toward the filter septum and because the relative motion between large particles and fine particles generates an appreciable upward velocity of liquid. This upward flow hinders the settling of fine particles; thus, the falling rate of each interface is slowed down. In the cases of mono-sized particle suspensions of ω = 100 and ω = 0, the lack of an extra hindered effect between large and fine particles causes these interfaces to fall faster than do those of a dual-sized dispersed suspension.

Variation of Solid Compressive Pressure

Figure 6 shows an example of the variations of the solid compressive pressure acting on the septum, P_{S1}, with times for different values of ω and separation modes. The solid curves represent the variation of P_{S1} of the gravity

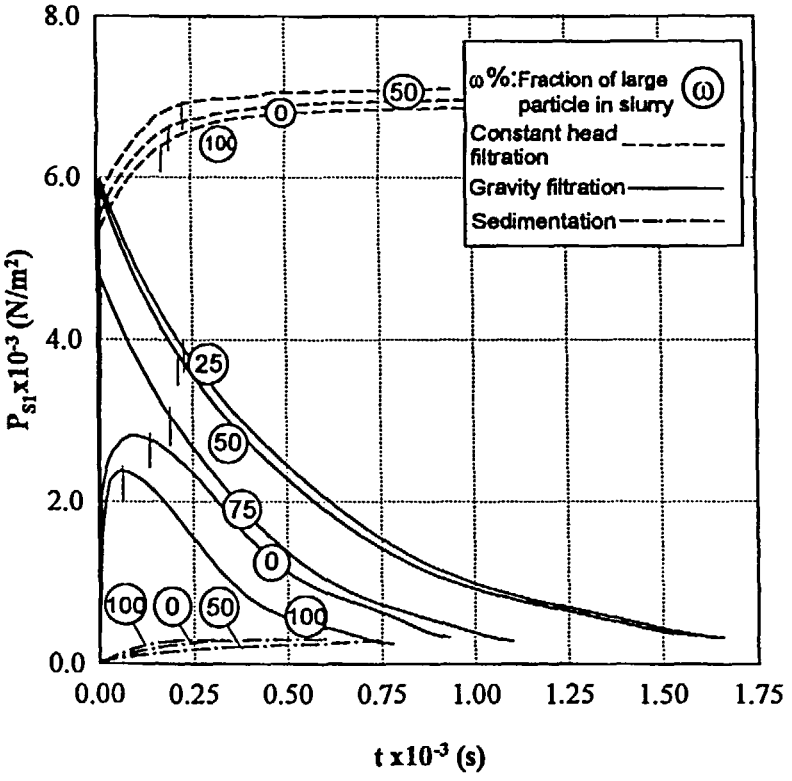

FIG. 6 Time course of P_{S1} for different ω and filtration modes. A vertical line (|) denotes the end of cake formation.

filtrations and the dashed curves show similar results for constant head filtrations. For a test run of gravity filtration, the value of P_{S1} increases sharply at the beginning of filtration until it reaches a maximum value and then decreases gradually. In a constant head filtration, the values of P_{S1} increase rather slowly during cake formation and reach a leveling off value at the end of cake formation. However, in sedimentation, the effective solid compressive pressure on each layer is the result of the downward force of the buoyed weight of the particles minus the upward force of friction due to the Darcian flow of liquid. In this figure the values of P_{S1} in the sediment were evaluated using the method proposed by Wakeman and Holdich (14). They are too small to be compared with those in the filter cake formed either by gravity filtration or by constant head filtration.

The convex-type pressure distribution behavior shown in a plot of P_{S1} vs t in gravity filtration is similar to the distributions encountered in centrifugal filtration (15). P_{S1} in a filtration process can be given as

$$P_{S1}(t) = P(t) - \mu q_1(t) R_m \tag{17}$$

in which the second term on the right-hand side is the pressure drop through the filter septum and R_m is the filtration resistance of the septum. Although the available head, $P(t)$, has a high value at the beginning of gravity filtration, the flow rate through the filter media, $q_1(t)$, is also large; as a result, the value of the difference of $P(t)$ and $\mu q_1(t) R_m$ on the RHS of Eq. (17) does not reach a maximum value at the beginning. As filtration proceeds, the cake builds up; thus, the magnitude of $\mu q_1(t) R_m$ drops faster than does the magnitude of the driving head, $P(t)$. This trend causes P_{S1} to continue to increase until it reaches a maximum. The end of cake formation, as the vertical line indicates in each curve in Fig. 6, becomes a pure permeation period. During this period the value of the driving head, $P(t)$, drops faster than does the value of the pressure drop through the filter medium, $\mu q_1(t) R_m$. Thus, the value of P_{S1} decreases gradually. This phenomenon is more evident for materials having high permeability.

As shown in Fig. 6, all the P_{S1} curves of the dual-dispersed suspensions lie above those of the mono-dispersed suspensions. This reveals that the cake structures formed by dual-sized particles have a higher solid compressive force than do those formed by monosized particles. For dual-dispersed suspensions, the higher the mixing ratio of large particles, the lower the P_{S1} value will be. This mainly occurs because the suspension with more large particles (large ω) forms a filter cake with a loose structure while a suspension with more fines will form high flow-resistance cake.

Figure 7 shows the variation of the local solid compressive pressure distributions P_S vs time during the course of gravity filtration for a mono-dispersed system. Since the effective solid compressive pressure P_S is zero at the cake surface and increases to its maximum value at the bottom of the filter cake, in this case P_{S1} reaches a maximum at $t = 125$ seconds before the end of cake formation. After $t = 165$ seconds, all the particles complete cake formation and liquid starts to permeate through the cake. During permeation the liquid level decreases and the value of P_S decreases with time. The cake thickness remains constant as the value of P_S decreases because the porosity is assumed to be an irreversible function of the effective solid compressive pressure reached at any time during the filtration process. It should be noted that this assumption is not valid for a filter cake composed of deformable particles. On the other hand, all the simulations stopped as the liquid level

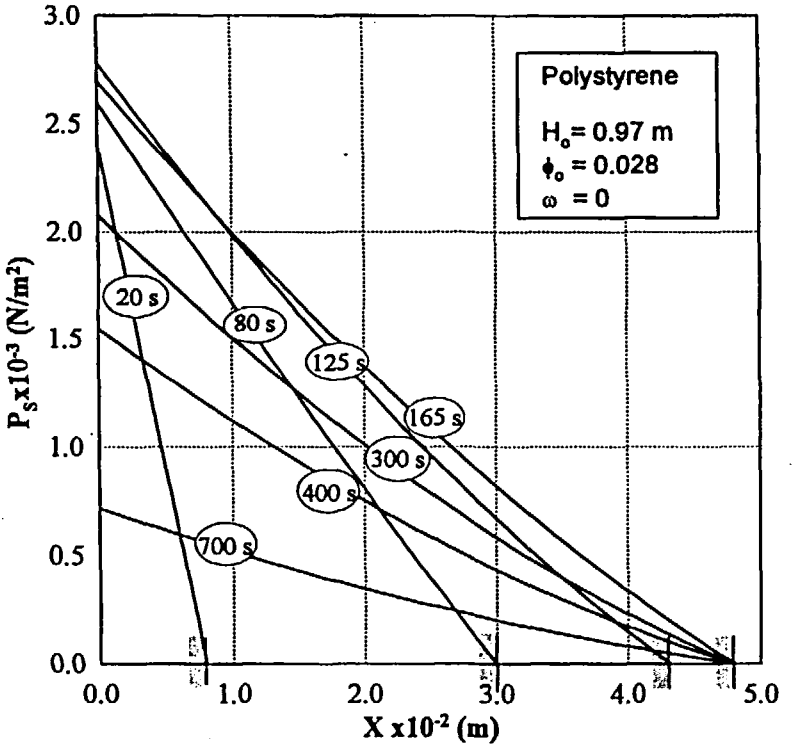

FIG. 7 Time course of the variation of the local solid pressure P_S distribution in cake. Shaded area and vertical line combinations denote the cake surface.

fell at the cake surface; Therefore, the dehydration of filter cakes is not considered in this study.

Porosity and Specific Filtration Resistance of Filter Cake

Figure 8 shows the simulated porosity distributions within filter cakes for different mixing ratios of slurry as the liquid level falls at the cake surface. The porosity near the filter septum of gravity filtration shows a convex behavior while that of constant head filtration shows a concave tendency. This discrepancy is mainly due to the change in the driving head during the filtration process. The sharp decrease in the porosity profile near the filter septum of gravity filtration implies that the compaction of the cake structure only occurs at the beginning of filtration due to the higher liquid head; then, as the liquid head falls and the solid compressive pressure decreases, the cake

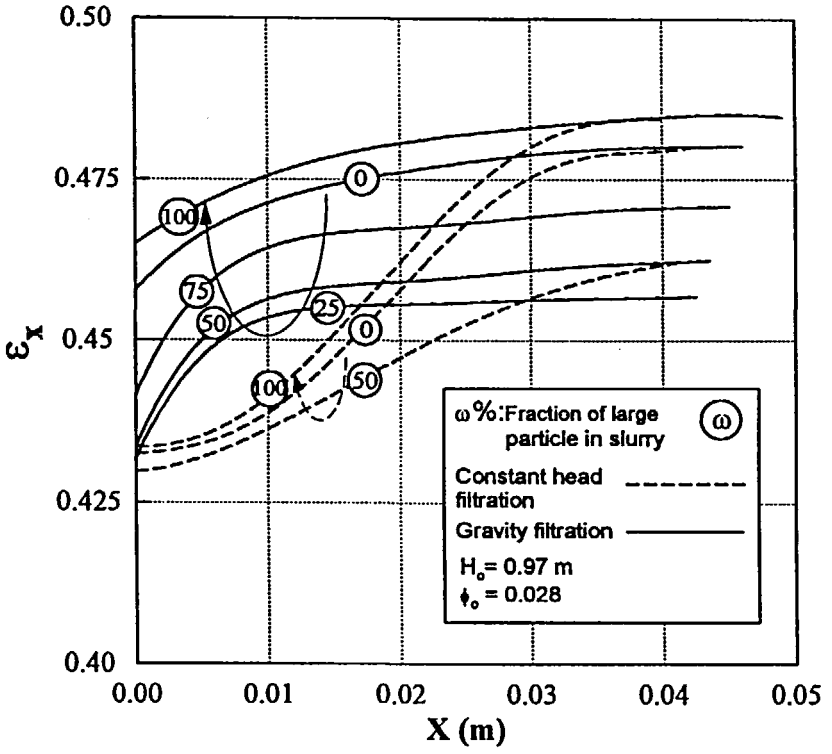

FIG. 8 Local porosity ϵ_x distribution in filter cake for different ω and filtration modes.

structure undergoes a negligible change near the surface of the cake. In contrast, a sharp decrease in the porosity profile is observed near the cake surface in a constant head filtration, which indicates that compaction of the cake structure occurs in this region in constant head filtration. All the porosity distribution curves of the dual-dispersed suspensions lie below those of the mono-dispersed suspensions owing to the cavern effect, which reduces the void within the cake. Thus, the cake structures formed by dual-sized particles are more compact as compared with those formed by mono-sized particles. For dual-dispersed suspensions, a larger mixing ratio of large particles will result in a larger local porosity and a thicker cake.

Figure 9 shows the distributions of the local specific filtration resistance, α, for various values of ω and filtration modes as the liquid level falls at the cake surface. One can find from Eq. (12) that the value of α is mainly affected by porosity and kS_0^2 (or d_p). In the region near the cake surface, α remains

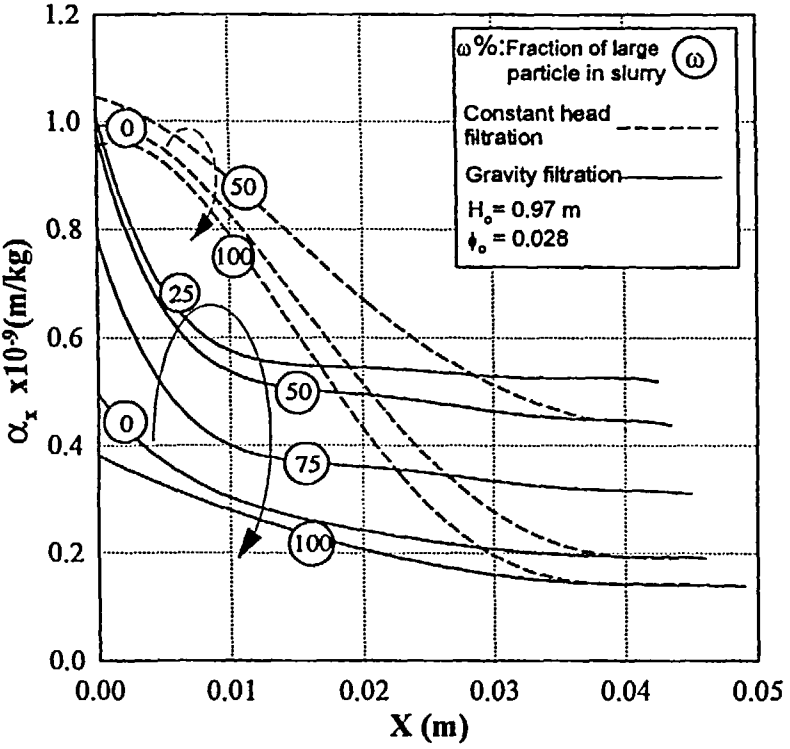

FIG. 9 Local specific resistance α_x distribution in filter cake for different ω and filtration modes.

nearly constant due to the same tendency of ϵ in gravity filtration. The value of α increases sharply toward the filter septum due to the sharp decrease of ϵ near the filter septum in gravity filtration. Furthermore, for dual-dispersed suspensions, the larger ω is, the larger is ϵ and the smaller is kS_0^2 (or larger is d_p), which results in a smaller α.

Particle Size Distribution in Formed Cake

Figure 10 shows comparisons of the particle size distributions (PSD) within cakes formed under constant head filtration, gravity filtration, and sedimentation. Since large particles always move faster than do fine particles toward the filter septum, a nonhomogeneous cake will be formed in gravity filtration, constant head filtration, and sedimentation. It can be observed in this figure

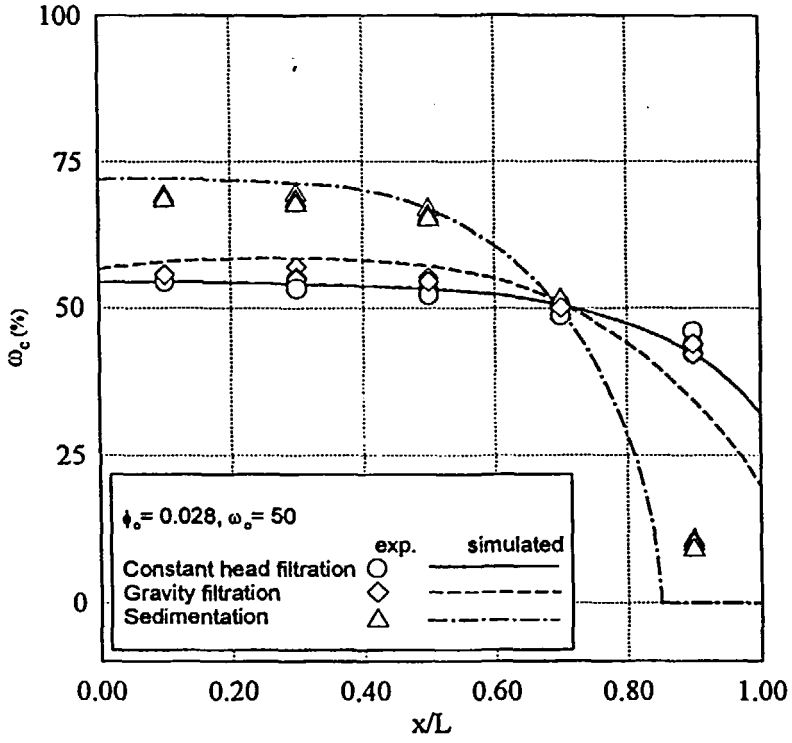

FIG. 10 Effects of separation modes on the particle size distribution in formed cake.

that the particle size distribution within a cake formed under constant head filtration is the most uniform one while that formed under sedimentation is the least uniform under the same initial slurry composition. This is mainly due to fluid flow toward the septum, which reduces the relative settling velocity between large particles and fine particles. The increase of the difference of the settling velocity between large particles and fine particle enlarges the nonuniformity of PSD within formed cakes. Because of the lack of fluid flow through the sediment toward the bottom of the sediment, the sedimentation process has the largest difference of settling velocity between large particles and fine particles. Thus, the most nonuniform cake is formed. Comparison of experimental and simulated values shows that the predicted results of particle size distribution in the formed cake agree well with the available experimental data.

CONCLUSION

The mechanism of simultaneous cake formation by particles in gravitational sedimentation and filtration has been studied. The dynamic analysis proposed by Lu and Hwang (7) has been applied to evaluate the local cake properties formed under a falling head. The effect of the particle size distribution on the local cake properties, such as the solid compressive pressure, porosity, and specific filtration resistance, have been thoroughly discussed. Both mono- and dual-sized dispersion slurries were used in this study, and the results have been compared with results obtained under sedimentation and constant head filtration for the same slurries. The results show that at a given position in a cake, the solid compressive pressure reaches a maximum value and then decreases for gravity filtration. A dual-dispersed suspension with a lower fraction of large particles will result in the lowest cake porosity and the highest specific filtration resistance of cake. The porosity near the filter septum of gravity filtration shows a convex behavior while that of constant head filtration shows a concave tendency. This discrepancy is mainly due to the change in the driving head during the filtration process. Furthermore, the predicted results of particle size distribution in the formed cake agreed well with the experimental data. Comparison of particle size distributions (PSD) within cakes formed under constant head filtration, gravity filtration, and sedimentation reveals that the uniformity of PSD in a filter cake is much better when the relative settling velocity between large particles and fine particles diminishes.

NOMENCLATURE

d_p	diameter of particles (m)
d^*	effective mean volume-surface-length diameter of particles in slurry column (m)
D	diameter of slurry column (m)
$f(\phi)$	hindered settling factor (—)
g	gravitational acceleration (m/s^2)
H_0	initial slurry head (m)
H_L	height of clear liquid (m)
H_S	slurry head (m)
k	Kozeny constant (—)
L	cake thickness (m)
m	mass ratio of wet to dry cake (—)
n	variable of summation (—)
P	hydrostatic pressure (Pa)
P_S	solid compressive pressure (Pa)
P_{S1}	solid compressive pressure on the filter septum (Pa)

ΔP_c	pressure drop across filter cake (Pa)
ΔP_m	pressure drop across filter medium (Pa)
ΔP_t	total driving pressure in gravity filtration (Pa)
q	filtration rate ($m^3/m^2 \cdot s$)
R_m	filtration resistance of filer medium (1/m)
s	mass fraction of solid in slurry (—)
S_0	specific surface area of particles (m^3/m^2)
t	filtration time (s)
u	settling velocity of particles in slurry column (m/s)
U	hindered settling velocity of particles in quiescent liquid (m/s)
U_0	Stokes' velocity of particles (m/s)
v	filtrate volume (m^3)
w_l	liquid weight per unit area (kg/m^2)
w_s	solid weight per unit area (kg/m^2)
x	distance from the surface of filter medium to the cake surface (m)

Greek Letters

α	specific filtration resistance (m/kg)
α_i	specific filtration resistance at the cake surface (m/kg)
β	hindered settling coefficient (—)
ϵ	porosity (—)
ϵ_i	porosity at the cake surface (—)
μ	fluid viscosity ($kg/m \cdot s$)
ρ_m	slurry density (kg/m^3)
ρ_s	particle density (kg/m^3)
σ	standard deviation of particle size distribution (m)
ϕ	volume fraction of particles in slurry column (—)
φ	mass fraction of particles of size d_p in the filter cake. (—)
ω	weight percent of large particles (%)

Subscripts

0	initial values
1	properties at the bottom of filer cake (i.e., properties at the surface of filter septum)
av	average value of properties of filter cake
i	at time $t = t_i$; properties at the surface of filter cake
j	the jth cake layer; $j = 1$, the cake layer at the bottom of filter cake; $j = i$, the cake layer at the surface of filter cake
t	at time t
x	local properties of filter cake

ACKNOWLEDGMENT

The authors wish to express their sincere gratitude to the National Science Council of the Republic of China for its financial support.

REFERENCES

1. F. M. Tiller, N. B. Hsyung, and S. L. Tarng, "Fluidization of Compatible Beds and Determination of Permeability and Porosity of Sediments Encountered in Thickening," *Liquid-Solid Flows* (ASME Symposium Series, edited by M. C. Roco, Vol. FEB-189), 1994, pp. 215–223.
2. A. Rushton, "Sedimentation Effect in Filtration," *Filtr. Sep, 10*, 267–272 (1973)
3. F. Bockstal, L. Fouarge, J. Hermia, and G. Rahier, "Constant Pressure Cake Filtration with Simultaneous Sedimentation," *Ibid.*, pp. 255–257 (July/August 1985).
4. H. Theliander "On the Influence of Settling of Particles in Filtration Tests—An Experimental Study," *Proceeding of Filtech '91 Conference, Vol. 1, Karlsruhe, Germany*, 1991, pp. 339–351.
5. F. M. Tiller, N. B. Hsyung, and D. Z. Cong, "Role of Porosity in Filtration: XII. Filtration with Sedimentation," *AIChE J., 41*(5), 1153–1164 (1995).
6. H. L. Nguyen, "Gravity Filtration with a Falling Head," *Fluid/Part. Sep. J., 5*, 75–81 (1992).
7. W. M. Lu and K. J. Hwang, "Mechanism of Cake Formation in Constant Pressure Filtrations," *Sep. Technol., 3*, 122–132 (1993).
8. W. G. B. Mandersloot, K. J. Scott, and C. P. Geyer, "Sedimentation in the Hindered Settling Regime," in *Advances in Solid-Liquid Separation* (H. S. Muralidhara, Ed.), Battelle Press, Columbus, OH, 1986, Chap. 3.
9. W. M. Lu, K. L. Tung, and K. J. Hwang, "Effect of Woven Structure on Transient Characteristics of Cake Filtration," *Chem. Eng. Sci., 52*(11), 1743–1756 (1997).
10. J. Happel and H. Brenner, *Low Reynolds Number Hydrodynamics*, Prentice-Hall, Englewood Cliffs, NJ, 1965, Chap. 8.
11. F. M. Tiller and M. Shirato, "The Role of Porosity in Filtration: VI. New Definition of Filtration Resistance," *AIChE J., 10*(1), 61–67 (1964).
12. S. Haynes Jr., "Flow through Compressible Porous Media Short-time Filtration, Wall Friction in Compression-Permeability Cells, and Rheological Models," Ph.D. Dissertation, University of Houston, Houston, Texas, 1966.
13. W. M. Lu, "Theoretical and Experimental Analysis of Variable Pressure Filtration and the Effect of Side Wall Friction in Compression-Permeability Cells," Ph.D. Dissertation, University of Houston, Houston, Texas, 1968.
14. R. J. Wakeman and R. G. Holdich, "Theoretical and Experimental Modeling of Solids and Liquid Pressures in Batch Sedimentation," *Filtr. Sep.*, pp. 420–422 (November/December 1984).
15. M. Sambuichi, H. Nakakura, K. Osasam, and F. M. Tiller, "Theory of Batchwise Centrifugal Sedimentation," *AIChE J., 33*(1), 109–120 (1987).

Received by editor August 21, 1997
Revision received December 1997